

Adenosine A_{2A} receptor imaging with [¹¹C]KF18446 PET in the rat brain after quinolinic acid lesion: Comparison with the dopamine receptor imaging

Kiichi ISHIWATA,* Nobuo OGI,** Nobutaka HAYAKAWA,** Keiichi ODA,* Tsukasa NAGAOKA,** Hinako TOYAMA,*† Fumio SUZUKI,**** Kazutoyo ENDO,** Akira TANAKA** and Michio SENDA*††

*Positron Medical Center, Tokyo Metropolitan Institute of Gerontology

**Showa Pharmaceutical University

***Tokyo Medical and Dental University

****Pharmaceutical Research Institute, Kyowa Hakko Kogyo Co., Ltd.

We proposed [¹¹C]KF18446 as a selective radioligand for mapping the adenosine A_{2A} receptors being highly enriched in the striatum by positron emission tomography (PET). In the present study, we investigated whether [¹¹C]KF18446 PET can detect the change in the striatal adenosine A_{2A} receptors in the rat after unilateral injection of an excitotoxin quinolinic acid into the striatum, a Huntington's disease model, to demonstrate the usefulness of [¹¹C]KF18446. The extent of the striatal lesion was identified based on MRI, to which the PET was co-registered. The binding potential of [¹¹C]KF18446 significantly decreased in the quinolinic acid-lesioned striatum. The decrease was comparable to the decrease in the potential of [¹¹C]raclopride binding to dopamine D₂ receptors in the lesioned striatum, but seemed to be larger than the decrease in the potential of [¹¹C]SCH 23390 binding to dopamine D₁ receptors. *Ex vivo* and *in vitro* autoradiography validated the PET signals. We concluded that [¹¹C]KF18446 PET can detect change in the adenosine A_{2A} receptors in the rat model, and will provide a new diagnostic tool for characterizing post-synaptic striatopallidal neurons in the stratum.

Key words: [¹¹C]KF18446, adenosine A_{2A} receptor, dopamine receptor, positron emission tomography, autoradiography

INTRODUCTION

ADENOSINE is an endogenous modulator of a number of physiological functions in the central nervous system (CNS) as well as in peripheral organs.^{1–3} Among four subtypes i.e., A₁, A_{2A}, A_{2B}, and A₃ receptors in the CNS, adenosine A₁ receptors exhibit a higher affinity for adenosine and inhibit adenylyl cyclase, and are present both pre- and post-synaptically in many regions, being rich in the hippocampus, cerebral cortex, thalamic nuclei, the

basal ganglia and the cerebellar cortex.^{4–8} Adenosine A_{2A} receptors exhibit a lower affinity for adenosine, stimulate adenylyl cyclase and are highly enriched in the striatum, nucleus accumbens and olfactory tubercle, in which dopamine D₁ and D₂ receptors are localized at very high densities.^{8–10} The *in situ* hybridization technique has demonstrated co-expression of adenosine A_{2A} receptor mRNA and dopamine D₂ receptor mRNA mainly in striatopallidal γ -aminobutyric acid (GABA)-ergic-enkephaline neurons.^{11–14}

A limited number of post-mortem human studies on the adenosine A_{2A} receptors have been reported. In patients with Huntington's disease in which selective degeneration of the striatopallidal neurons is one of the pathological features, the adenosine A_{2A} receptor density is significantly reduced in the striatum.^{15,16} A loss of adenosine A_{2A} receptor binding in the caudate nucleus, putamen and external globus pallidus was more predominant than that of dopamine D₂ receptor binding.¹⁶ In patients with

Received March 6, 2002, revision accepted July 29, 2002.

Present address: †National Institute of Radiological Sciences, Chiba, Japan; and ††Institute of Biomedical Research and Innovation, Kobe, Japan.

For reprint contact: Kiichi Ishiwata, Ph.D., Positron Medical Center, Tokyo Metropolitan Institute of Gerontology, 1–1, Naka-cho, Itabashi, Tokyo 173–0022, JAPAN.

E-mail: ishiwata@pet.tmig.or.jp

Parkinson's disease characterized by selective degeneration of nigrostriatal dopamine neurons, the adenosine A_{2A} density is not significantly affected.¹⁵ On the other hand, a significant decrease in the level of adenosine A_{2A} receptor mRNA was found in the anterior and posterior caudate nucleus and anterior dorsal putamen of the patients who died of Parkinson's disease and who were receiving treatment with dopaminergic drugs, whereas a significant increase was observed in the substantia nigra pars reticulata when compared to age-matched controls.¹⁷ In the post-mortem brain of the schizophrenic patients, there was a significant increase in the specific binding of adenosine A_{2A} selective [³H]CGS21680 in the putamen and caudate, but not in the globus pallidus of the externa, compared to those of controls.¹⁸ Therefore, positron emission tomography (PET) with selective radioligands has the potential to investigate the physiological roles of the adenosine A_{2A} receptors in the human brain, and can provide a new diagnostic tool for neurological and psychiatric disorders.

Based on the these backgrounds, we have proposed several positron-emitting ligands for mapping the CNS adenosine A_{2A} receptors.^{19–24} Among them, [¹¹C]KF18446^{21,22} {[7-methyl-¹¹C]-(*E*)-8-(3,4,5-trimethoxystyryl)-1,3,7-trimethylxanthine} and [¹¹C]KF21213²⁴ {[7-methyl-¹¹C]-(*E*)-8-(2,3-dimethyl-4-methoxystyryl)-1,3,7-trimethylxanthine} have promising properties as PET ligands. [¹¹C]KF18446 has been successfully applied to the imaging of the adenosine A_{2A} receptors in the monkey striatum by PET.²¹ In the present study, to demonstrate the usefulness of [¹¹C]KF18446, we investigated whether [¹¹C]KF18446 PET can detect the change in adenosine A_{2A} receptors in a rat model of Huntington's disease, in which quinolinic acid, an excitotoxin, was injected into the striatum to degenerate dopaminergic neurons. We also compared the degeneration of dopamine D₁ and D₂ receptors in the same rat model. *Ex vivo* and *in vitro* autoradiography was also performed to validate the PET signals. The rat model used has been well established.^{25–29} Although the rat brain is small for quantitative PET measurement, the changes in dopamine D₂ receptors in the rat model were semi-quantitatively evaluated.^{30,31}

MATERIALS AND METHODS

Materials

2-Chloroadenosine, cis-(z)-flupentixol, haloperidol hydrochloride and ketanserin were purchased from Research Biochemical, Inc. (Natick, MA, USA). Quinolinic acid was purchased from Sigma (St. Louis, MO, USA). Adenosine diaminase was purchased from Boehringer Mannheim (Indianapolis, IN, USA). Other chemicals were purchased from Wako Pure Chemical Industries (Tokyo, Japan).

Radiosynthesis of [¹¹C]KF18446,²¹ [¹¹C]SCH 23390,³²

[¹¹C]raclopride³³ and [¹¹C]flumazenil³⁴ was carried out by ¹¹C-methylation of the respective demethyl compound as described previously.

Quinolinic acid-lesioned rats

Male Wistar rats were obtained from Tokyo Laboratory Animals Company (Tokyo, Japan). The animal studies were approved by the Animal Care and Use Committee of Tokyo Metropolitan Institute of Gerontology.

The rat model for the degeneration of striatal striato-pallidal neurons was prepared by intrastratial injection of quinolinic acid as described previously.^{27,30} Briefly, the rat (8–10 weeks old) was anesthetized with pentobarbital (50 mg/kg, i.p.) and the head was positioned in a stereotaxic frame. The quinolinic acid solution (500 nmol in 2 μ l) in 0.1 M phosphate buffer (pH 7.2) was infused into the right striatum at the coordinates AP = + 0.0 mm, L = + 3.0 mm, V = + 4.0 mm from the bregma in the atlas of Paxinos and Watson³⁵ over a 10-min period by using a micro-infusion pump. Five days after the treatment, a total of 26 rats weighing 199 \pm 50 g were used in the experiments described below. Nine rats weighing 295 \pm 36 g were used as the control after treatment with the phosphate buffer without quinolinic acid in the same manner.

PET study

PET measurement was performed in 12 quinolinic acid-treated rats and in six control rats with a model SHR-2000 camera (Hamamatsu Photonics K.K., Hamamatsu, Japan) as described previously.^{30,31,36,37} The camera provides a set of 14-slice images at center-to-center intervals of 3.25 mm with an image spatial resolution of 4.0 mm full width at half maximum and an axial resolution of 5.0 mm full width at half maximum. Each rat was anesthetized with isoflurane (2.0%) and was positioned prone on a stereotaxic head holder. After a transmission scan to correct for photon attenuation, the ¹¹C-labeled ligand was injected through the tail vein via a catheter and a time sequential tomographic scan was performed for 60 min (20 frames by 30 sec and 50 frames by 1 min). Up to three radioligands, in the order [¹¹C]KF18446, [¹¹C]raclopride and [¹¹C]SCH 23390, were given at 90–120 min intervals, and the PET scanning was successively performed on the same animals. Because the half-life of ¹¹C was 20 min, the residual radioactivity was negligible in the succeeding PET measurements. In two quinolinic acid-treated rats that had an MRI scan as described below, PET measurement with [¹¹C]flumazenil (n = 2) was performed last to acquire data for PET-MRI registration. Altogether seven quinolinic acid-treated rats were scanned for each of the three radioligands. Three, 5 and 4 of the six control rats were scanned with [¹¹C]KF18446, [¹¹C]SCH 23390 and [¹¹C]raclopride, respectively. Injected doses of radioligands were 9.9 \pm 0.8 MBq/0.33 \pm 0.08 nmol for [¹¹C]KF18446, 10.6 \pm 1.7 MBq/0.48 \pm 0.33 nmol for [¹¹C]SCH 23390, 10.7 \pm 0.8 MBq/0.46 \pm 0.24 nmol for

[¹¹C]raclopride and 11 MBq/0.19 or 0.13 nmol for [¹¹C]flumazenil. To measure the radioactivity in the striatum and cerebellum, regions of interest (ROIs) were placed based on early PET images, a stereotaxic atlas of the rat brain³⁵ and the MRI images prepared below. The striatal ROI with 25 mm² was placed on the bregma slice. The cerebellar ROI (60 mm²) was placed on the slice at a distance of 9.75 mm from the bregma. The decay-corrected radioactivity value was expressed as the percentage of the injected dose per ml of tissue volume (%ID/ml).

To evaluate the partial volume effect on the activity in the ROIs, PET measurement also performed with two plastic tubes of 3.1 mm and 9.6 mm inside diameter (i.d.) as phantoms for the striatum and cerebellum, respectively. We also used the other tube with 13.1 mm i.d. that is taken as the cerebral cortex. At the center of the tube, two tubes of 3.1 mm i.d. were set at a distance of 2.0 mm apart as a couple of striata. The wall thickness of the 3.1-mm tube was 0.1 mm, and all tubes were approximately 5 cm long. PET measurement was carried out at the concentrations of 0.43 MBq/ml in the 3.1-mm phantom and of 0.086 MBq/ml in the 9.6-mm and 13.1-mm phantoms, and the radioactivity was measured in the 25-mm² and 60-mm² ROIs placed on the 3.1-mm and 9.6-mm phantoms, respectively.

The kinetic analysis of the binding of [¹¹C]KF18446, [¹¹C]SCH 23390 or [¹¹C]raclopride to striatal receptors was performed according to the method described by Hume et al. based on the reference tissue model,³⁸ in which the striatal radioactivity was composed of free ligand and receptor-bound ligand. The concentration of the striatal free ligand was assumed to be equal to the radioactivity in the cerebellum, and the receptor-bound ligand was assessed as the difference between the total radioactivity in the striatum and that in the cerebellum. The association and dissociation rate constants were estimated by means of a non-linear least squares fitting procedure with the free ligand as the input, and their ratio, which represents the binding potential of ¹¹C-labeled ligand to striatal receptors, was calculated.

MRI scanning and PET-MRI image registration

Two quinolinic acid-treated rats had MRI under isoflurane inhalation anesthesia the day prior to the PET study as previously described.³⁷ The MRI scan was carried out on a 4.7 Tesla experimental imager/spectrometer system (Unity plus SIS 200/330, Varian, PaloAlto, CA, USA). T2-weighted images were obtained perpendicular to the base of the brain.

PET imaging of the two rats was carried out with [¹¹C]flumazenil and with the three other radioligands as described above. Based on the [¹¹C]flumazenil PET, the PET images of the other three radioligands were registered to the MRI images by the method of Ardekani et al.,³⁹ which has been slightly modified to apply to the rat

brain by Hayakawa et al.³⁷

Ex vivo autoradiography

Ex vivo autoradiography was performed with imaging plates and a type BAS 2500 bioimaging analyzer (Fuji Photo Film Co., Ltd., Tokyo, Japan) in 12 quinolinic acid-treated rats as previously described.⁴⁰ The rats were killed 30 min postinjection of each radioligand (n = 3). Injected doses of radioligands were 180 ± 19 MBq/4.2 ± 0.8 nmol for [¹¹C]KF18446, 100 ± 14 MBq/3.8 ± 0.4 nmol for [¹¹C]SCH 23390 and 94 ± 12 MBq/3.2 ± 1.4 nmol for [¹¹C]raclopride. The brain was quickly removed, and coronal brain sections 20-μm thick were dried on a hot plate at 60°C and exposed on imaging plates. The radioligand distribution was visualized, and the symmetrical ROIs were placed on the entire striatal regions of both hemispheres based on the histological images of the brain sections. The total binding ratio of lesioned striatum to non-lesioned striatum was calculated.

In vitro autoradiography

In vitro autoradiography was performed in nine quinolinic acid-treated rats and three control rats. Three of the nine quinolinic acid-treated rats had undergone *ex vivo* autoradiography with each of the three tracers as described above. The other six had only *in vitro* autoradiography. All the three control rats had undergone PET measurement. The brain was frozen and coronal brain sections 20-μm thick were prepared immediately or after storage at -80°C. Within two days after preparation of the brain sections, *in vitro* autoradiography was carried out as described previously.⁴⁰

The binding assay for adenosine A_{2A} receptors and dopamine D₁ and D₂ receptors was carried out according to the slightly modified method of Levivier et al.²⁷ For adenosine A_{2A} receptor binding, brain sections were pre-incubated in 50 mM Tris-HCl, pH 7.4, containing 10 mM MgCl₂ and 0.2 IU/mL adenosine deaminase for 30 min at room temperature. Then the sections were incubated in the same buffer containing 2.4 ± 0.7 nM (100 kBq/mL) [¹¹C]KF18446 with and without 20 μM 2-chloroadenosine for 60 min at 4°C. For dopamine D₁ receptors binding, brain sections were pre-incubated in 50 mM Tris-HCl, pH 7.4, containing 120 mM NaCl, 5 mM KCl, 2 mM CaCl₂, 1 mM MgCl₂ for 10 min at room temperature. Then the sections were incubated in the same buffer containing 4.2 ± 1.9 nM (100 kBq/mL) [¹¹C]SCH 23390 and 50 nM ketanserin with and without 20 μM cis-(z)-flupentixol for 30 min at 37°C. For dopamine D₂ receptor binding, brain sections were pre-incubated in 50 mM Tris-HCl, pH 7.4, containing 120 mM NaCl for 10 min at room temperature. Then the sections were incubated in the same buffer containing 2.2 ± 0.6 nM (100 kBq/mL) [¹¹C]raclopride with and without 20 μM haloperidol for 25 min at room temperature.

After the binding assay, the brain sections were washed

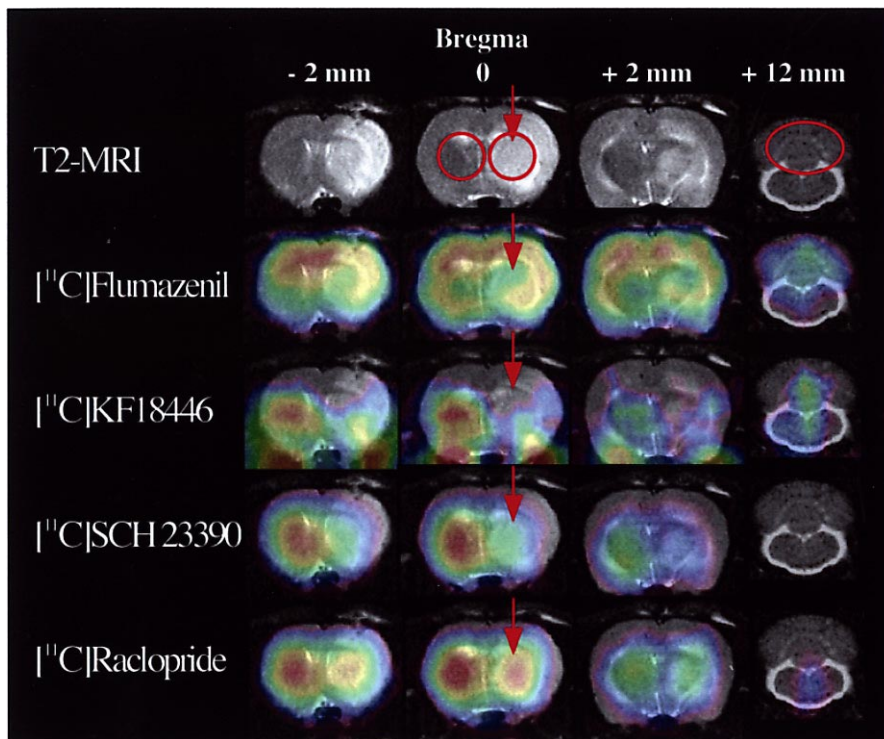


Fig. 1 Brain PET-MRI registration image of the quinolinic acid-lesioned rat scanned with [^{11}C]flumazenil, [^{11}C]KF18446, [^{11}C]SCH 23390 and [^{11}C]raclopride. Four PET scans were carried out in the order of [^{11}C]KF18446, [^{11}C]raclopride, [^{11}C]SCH 23390 and [^{11}C]flumazenil in the same individual. The images were acquired from 20 min to 40 min postinjection for [^{11}C]flumazenil and [^{11}C]raclopride, from 10 min to 30 min postinjection for [^{11}C]KF18446 and from 30 min to 60 min postinjection for [^{11}C]SCH 23390.

with ice-cold 50 mM Tris-HCl, pH 7.4, for 5 min, dipped in ice-cold distilled water, dried on a hot plate at 60°C, and apposed on an imaging plate. The tracer distribution was visualized and the ROI was placed on the striatum, and the binding ratio of lesioned striatum to non-lesioned striatum was calculated in the same manner as in the *ex vivo* autoradiography.

RESULTS

PET study

Figure 1 shows PET and MRI images of the quinolinic acid-lesioned rat brain. The PET images were superimposed on the MRI by the registration technique which utilized [^{11}C]flumazenil-PET.^{37,39} In the MRI images of the quinolinic acid-lesioned rat, a hyperintense area spread in the quinolinic acid-lesioned hemisphere. The three ligands all showed a lower uptake on the quinolinic acid-lesioned side than on the normal side. The reduced uptake of [^{11}C]KF18446 and [^{11}C]SCH 23390 was visualized more prominently than that of [^{11}C]raclopride. In the case of [^{11}C]KF18446, extracranial radioactivity was also observed. At the bregma the extracranial radioactivity clearly covered a part of the cortical region and may affect the striatal activity, especially on the quinolinic acid-lesioned

side. In the phosphate buffer-injected control rats, PET with each of the three radioligands clearly showed the striatum images with bilateral symmetry (not shown).

Figure 2 represents the time-activity curves of the three radioligands in the striatum and cerebellum of the quinolinic acid-treated rat shown in Figure 1. The striatal activity of [^{11}C]SCH 23390 remained high for 60 min in the non-lesioned striatum, but gradually decreased on the quinolinic acid-lesioned side. The activity of [^{11}C]KF18446 and [^{11}C]raclopride decreased, and the levels were slightly lower on the lesioned side than on the non-lesioned side after 5 min. Compared with the time-activity curves of [^{11}C]raclopride, those of [^{11}C]KF18446 were very noisy, especially on the quinolinic acid-lesioned side, probably because of the extracranial activity.

In an experiment with three types of phantoms, when the 25-mm² ROI was placed on the 3.1-mm phantom with no activity outside, 45% of the total activity was recovered. The corresponding value was 44% on a 60-mm² ROI in the 9.6-mm phantom. Nevertheless, when the 25-mm² ROI was placed on the 3.1-mm phantom in the 13.1-mm phantom, recovery corresponded to 66% of the total activity (0.43 MBq/ml in the 3.1-mm tube and 0.086 MBq/ml outside) and 92% for 0.43 MBq/ml in the 3.1-mm tube.

As shown in Table 1, the binding potential on the

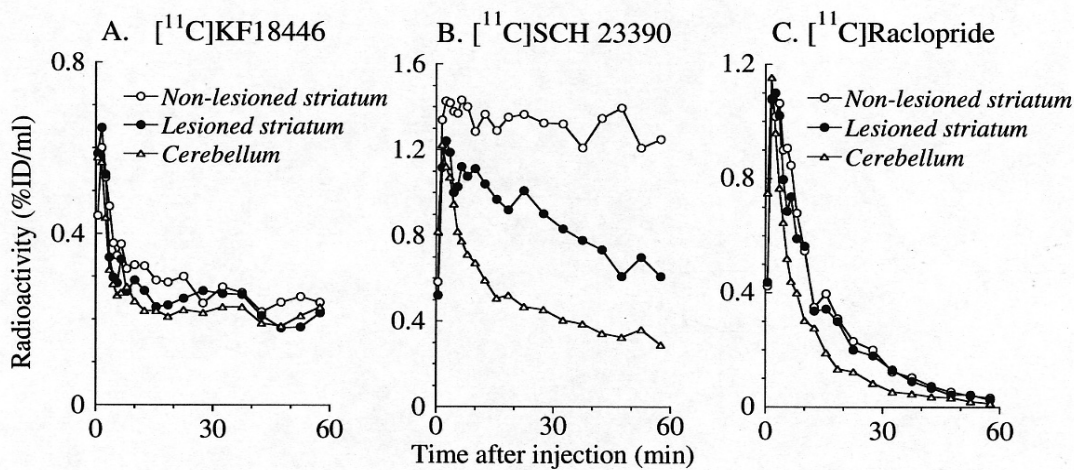


Fig. 2 Time-activity curves of [^{11}C]KF18446 (A), [^{11}C]SCH 23390 (B) and [^{11}C]raclopride (C) on the quinolinic acid-lesioned rat brain after intravenous injection of ^{11}C -labeled tracers. The time-activity curves were obtained from the same individual rat presented in Figure 1. Open circle, striatum of non-lesioned side; filled circle, striatum of quinolinic acid-lesioned side; and triangle, cerebellum.

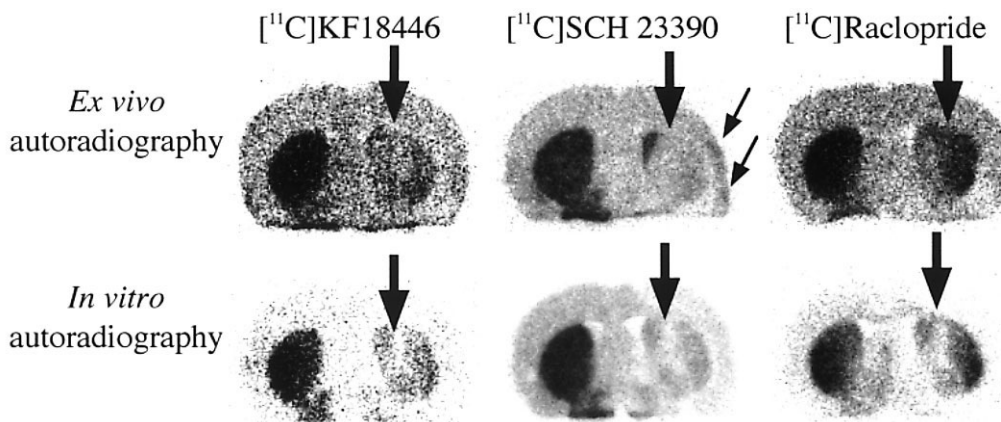


Fig. 3 *Ex vivo* and *in vitro* autoradiograms of the rat brain with [^{11}C]KF18446, [^{11}C]SCH 23390 and [^{11}C]raclopride. The *ex vivo* autoradiography was performed at 30 min after an intravenous injection of ^{11}C -labeled tracers. After decay-out of the radioactivity, the adjacent brain sections of the same rat were applied to *in vitro* autoradiography. Upper and lower lines show *ex vivo* autoradiograms and *in vitro* autoradiograms, respectively. Thick arrows indicate the side in which the probe was inserted to inject quinolinic acid, and thin arrows show the area presenting a slight accumulation of [^{11}C]SCH 23390 in the cerebral cortex.

non-lesioned side was the largest for [^{11}C]SCH 23390, followed by [^{11}C]raclopride and [^{11}C]KF18446. The quinolinic acid lesioning significantly decreased the binding potential of each of the three radioligands. In the control rats, the left-to-right ratios of the binding potential were 1.01 ± 0.01 ($n = 3$) for [^{11}C]KF18446, 0.98 ± 0.08 ($n = 5$) for [^{11}C]SCH 23390 and 1.01 ± 0.04 ($n = 4$) for [^{11}C]raclopride.

Ex vivo and in vitro autoradiography

To demonstrate the difference between *ex vivo* and *in vitro* autoradiography, images of the three radioligands in

the same individuals are shown in Figure 3. The binding of each radioligand significantly decreased ($p < 0.001$) on the lesioned striatum by both *ex vivo* and *in vitro* autoradiography, when compared to the non-lesioned striatum. The reduced binding area was widespread over the striatum for all the radioligands. Table 2 shows that the binding ratios of the lesioned side to non-lesioned side for [^{11}C]SCH 23390 were smaller than those for [^{11}C]raclopride and [^{11}C]KF18446 both *ex vivo* and *in vitro*. The *in vitro* binding ratios for all radioligands were approximately two-third of the *ex vivo* binding ratios. In the control rats, the *in vitro* binding ratios were 0.97 ± 0.05

Table 1 Binding potential of [¹¹C]KF18446, [¹¹C]SCH 23390 and [¹¹C]raclopride in the quinolinic acid-lesioned rat brain measured by PET

	Binding potential		
	Non-lesioned side	Lesioned side	Ratio*
[¹¹ C]KF18446	0.59 ± 0.11	0.43 ± 0.06 ^b	0.75 ± 0.13
[¹¹ C]SCH 23390	2.40 ± 0.36	1.58 ± 0.60 ^b	0.64 ± 0.18
[¹¹ C]Raclopride	0.79 ± 0.03	0.63 ± 0.09 ^a	0.75 ± 0.10

*Values are expressed as the ratios of binding potential in the treated side to that in the intact side. Mean ± s.d. (n = 7).

^aP < 0.001 and ^bp < 0.01 (Student's t-test, compared with non-lesioned side).

Table 2 Binding ratios of [¹¹C]KF18446, [¹¹C]SCH 23390 and [¹¹C]raclopride in the quinolinic acid-lesioned rat striatum measured by *ex vivo* and *in vitro* autoradiography

	Binding ratio*	
	<i>Ex vivo</i> autoradiography	<i>In vitro</i> autoradiography**
[¹¹ C]KF18446	0.54 ± 0.05 ^a	0.35 ± 0.08 ^a
[¹¹ C]SCH 23390	0.30 ± 0.05 ^a	0.21 ± 0.07 ^a
[¹¹ C]Raclopride	0.62 ± 0.10 ^a	0.43 ± 0.17 ^a

*Binding ratios of lesioned striatum to non-lesioned striatum are calculated from the total binding in *ex vivo* autoradiography and from the specific binding in *in vitro* autoradiography.

**Data obtained after *ex vivo* autoradiography were excluded. Mean ± s.d. (n = 4 for *ex vivo* autoradiography and n = 6 for *in vitro* autoradiography).

^aP < 0.001 (Student's t-test, compared with non-lesioned striatum).

for [¹¹C]KF18446, 0.96 ± 0.05 for [¹¹C]SCH 23390 and 0.97 ± 0.01 for [¹¹C]raclopride (n = 3), but the binding was scarcely affected in the brain section ± 1 mm from the bregma.

The *ex vivo* binding of [¹¹C]KF18446 and [¹¹C]raclopride in the cortex was not changed by the quinolinic acid lesioning, but [¹¹C]SCH 23390 slightly accumulated *ex vivo* in the forelimb area of the cortex, in which the probe was inserted to inject quinolinic acid, and in the cortex overlying the injured striatum. On the other hand, the *in vitro* binding of each radioligand in the same cortical region was slightly reduced.

DISCUSSION

In the present study we have demonstrated that [¹¹C]KF18446 PET can detect change in the adenosine A_{2A} receptors in a rat model of the Huntington's disease. It is well known that the striatal injection of excitotoxins such as quinolinic acid and kainic acid induces degeneration of post-synaptic neurons. *In vitro* autoradiography

and membrane binding assay of the rat brain have demonstrated degeneration of adenosine A_{2A} receptor and dopamine D₁ and D₂ receptors.^{25–29,41–43} Those reports show that the dopamine D₁ receptors are reduced more prominently than the dopamine D₂ receptors,^{27,42,43} and that the reduction in adenosine A_{2A} receptors is comparable to that in dopamine D₂ receptors.^{27,28} The striatonigral and striatoentopeduncular GABAergic neurons contain dopamine D₁ receptors,^{11,44,45} whereas dopamine D₂ receptor mRNA and adenosine A_{2A} receptor mRNA are colocalized in the striatopallidal GABAergic-enkephaline neurons.^{11–14} The present PET measurement showed that the binding potential for each radioligand significantly decreased, but no significant difference was found among three receptors, when compared to the ratio of the quinolinic acid-lesioned side to the non-lesioned side. We confirmed the location of the striatal lesion in two rats by the image registration technique with [¹¹C]flumazenil-PET and MRI.³⁷ The registration was able to be performed because the [¹¹C]flumazenil binding was not greatly affected by the quinolinic acid-lesioning, although the [¹¹C]SCH 23390 binding was differently affected *in vitro* and *ex vivo* in the cerebral cortex overlying the lesioned striatum, as described below.^{30,37} Furthermore, the PET signal was validated with both *ex vivo* and *in vitro* autoradiography.

In the present study we injected a supramaximal dose of quinolinic acid (500 nmol) into the striatum and evaluated the condition five day after the treatment²⁵ to certify detecting the changes in adenosine A_{2A} and dopamine receptors in a small animal model by PET, which showed the severe degeneration of the receptors investigated. Consequently, the susceptibility of the three neuroreceptors could not be clearly discriminated. Furthermore, the quantitative comparison of the changes in the three receptors may be problematic in the present rat model. In the case of [¹¹C]KF18446, a high accumulation of the radioactivity was found in the extracranial region (Fig. 1). No such radioactivity was found in [¹¹C]SCH 23390 or [¹¹C]raclopride, or in the case of the other adenosine A_{2A} ligand [¹¹C]KF21213.²⁴ The extracranial radioactivity of [¹¹C]KF18446 may be present in and around the salivary glands. The three radioligands also showed a high accumulation in and around the Harderian glands (not shown) as previously reported for [¹¹C]raclopride.³⁶ These activities may influence the radioactivity in the ROIs on the striatum and cerebellum because of the partial volume effect based on the small rat brain contrasted with the PET camera used. Indeed, the reduction in the [¹¹C]SCH 23390 binding and [¹¹C]KF18446 binding was not significantly different.

As for the partial volume effect, we carried out an experiment with three types of phantoms assuming the striatum only, cerebellum and cerebral cortex containing striata. The recovery yields in the 25 mm² and 60 mm² ROIs on the striatal and cerebellar phantoms, respectively, were comparable (45% and 44%), but the recovery

in the 25-mm² ROI was greatly increased inside the phantom of the cerebral cortex. The activity ratios for striatum to cerebral cortex were very different among three radioligands and changed with time, and also different from those of striatum to cerebellum: striatum-to-cerebral cortex uptake ratios, 2.7–2.5 [¹¹C]KF18446 (unpublished), 2.5–6.5 for [¹¹C]SCH 23390 (unpublished) and for 3.0–4.9 for [¹¹C]raclopride³⁶; and striatum-to-cerebellum uptake ratios, 2.0–2.1 [¹¹C]KF18446 (unpublished), 5.2–19.6 for [¹¹C]SCH 23390 (unpublished) and for 4.2–6.5 for [¹¹C]raclopride³⁶ in rats for 15–60 min after the tracer injection. Therefore, the appropriate correction for the partial volume effect was not carried out in the present study. These effects also make it hard to compare changes in the three receptors in the present rat model.

The diagnosis of neurological disorders by PET targeting adenosine A_{2A} receptors is of great interest. So far a large numbers of PET and SPECT studies have been performed to characterize degeneration of pre-synaptic nigrostriatal and post-synaptic striatopallidal neurons of the stratum in patients with neurological disorders.^{46–48} The pre-synaptic function was evaluated with the dopamine synthesis ability and the dopamine transporter density, whereas the post-synaptic function was usually evaluated with the density of dopamine D₂ receptors. Parkinson's disease is differentially diagnosed from other parkinsonian syndromes to a certain extent, but clinical variation in the symptoms, therapeutic response and prognosis of Parkinson's disease cannot be explained only by evaluating the metabolic profiles and dopaminergic system. Furthermore, parkinsonian syndromes such as multiple system atrophy, progressive supranuclear palsy, corticobasal degeneration and diffuse Lewy Body disease showed degeneration of post-synaptic as well as pre-synaptic dopaminergic functions,^{46–48} but PET and SPECT discrimination among each of the parkinsonian syndromes has been hardly established, so that the adenosine A_{2A} receptor can be used as a marker as the dopamine D₂ receptor, because both receptors are co-expressed on GABAergic–enkephaline neurons.^{11–14} Nevertheless, a number of studies including signal transduction, gene expression, neurotransmitter release and behavioral responses, showed that the adenosine A_{2A} receptors had opposite effects on dopamine D₂ receptor mediated-effects, although A_{2A}-D₂ receptor interaction was also suggested.⁴⁹ Therefore, [¹¹C]KF18446 PET may be an alternative diagnostic tool, being different from [¹¹C]raclopride PET, although the difference between the reduced binding of [¹¹C]KF18446 to adenosine A_{2A} receptors and the reduced binding of [¹¹C]raclopride to dopamine D₂ receptors was not significant probably because of the partial volume effect in the present rat model.

When PET and *ex vivo* and *in vitro* autoradiography were compared, degeneration of three receptors was visualized much more prominently with *in vitro* autoradiogra-

phy than with PET and with *ex vivo* autoradiography. First, it is pointed out that the binding ratios in the *in vitro* autoradiography were evaluated from specific binding while those in the *ex vivo* autoradiography were from the total binding (Table 2). Second, a distinct difference exists between *in vitro* and *in vivo* in terms of ligand delivery. The *in vitro* autoradiography data are acquired in the equilibrium state reflecting the maximal ligand-receptor binding, whereas the ligand is not in equilibrium with the receptors in PET and *ex vivo* autoradiography. As for the difference between the *ex vivo* autoradiography data and the PET data, one should also keep in mind that the PET data were quantitatively evaluated from the kinetics for 60 min, whereas the *ex vivo* autoradiography data were obtained qualitatively at a single time. In *ex vivo* autoradiography, free ligand may be withdrawn from the brain after decapitation. The PET striatum signal is much lower than the signal for radioactivity uptake directly recovered from the tissue sample because of the partial volume effect.

We applied two or three tracers to the same individuals for PET studies (Fig. 1) for comparison of the characteristics of three receptor radioligands, or performed *ex vivo* and *in vitro* autoradiography on the same individuals (Fig. 3) to demonstrate the difference between *ex vivo* and *in vitro*. To minimize the effect of proceeding experiments on subsequent PET measurements, a ligand with weaker affinity, i.e. [¹¹C]KF18446 or [¹¹C]raclopride, was investigated first, followed by higher affinity [¹¹C]SCH 23390. Because of the high-specific activity of the ligands used, we detected hardly any sign of remaining ligand molecules affecting the kinetics of the tracer in succeeding PET studies. Nevertheless, the results in the *ex vivo* autoradiography with [¹¹C]KF18446 (Table 2), the dose of which was more than 10 times larger (mean = 21 nmol/kg body weight) than the dose in PET studies (mean = 1.7 nmol/kg body weight), may be underestimated. We confirmed previously no significant decrease in the striatal uptake of [¹¹C]KF18446 until 8.5 nmol/kg in mice but a 12% reduction at 29 nmol/kg.²¹ In a comparative study of three dopamine D₂-like receptor ligands, [¹¹C]raclopride, [¹¹C]*N*-methylspiperone and [¹¹C]nemonapride, in the same animal model, the larger dose of [¹¹C]raclopride did not apparently change the PET image or the time-activity curve.³⁰ In *in vitro* autoradiography, no significant difference between the rats that had *ex vivo* autoradiography before and those that did not was found in the ratio of radioactivity on the lesioned side to that on the non-lesioned side.

An unexpected finding was an increased binding of [¹¹C]SCH 23390 *ex vivo* in the cerebral cortex overlaying the lesioned striatum, in spite of decreased binding *in vitro*. A similar phenomena was not clear for the binding of either [¹¹C]raclopride nor [¹¹C]KF18446, but found for the binding of the other two dopamine D₂-like receptor ligands, [¹¹C]*N*-methylspiperone and [¹¹C]nemonapride,

in the same rat model.³⁴ But the phenomena did not seem to substantially affect the PET measurement with [¹¹C]SCH 23390. It is well known that injection of excitotoxins into the brain causes marked gliosis and severe inflammation around the injection site.²⁹ Töpper et al. immunocytochemically detected microglial activation in these cortical areas as well as in the striatum after intrastriatal injection of quinolinic acid (240 nmol).²⁶ Kelly et al.⁵⁰ showed an increase (15%) of glucose utilization in the sensory-motor cortex after injection of kainic acid into the rat striatum by *ex vivo* autoradiography with [¹⁴C]deoxyglucose, suggesting inflammation.⁵¹

CONCLUSION

We have demonstrated that the binding of [¹¹C]KF18446 to the striatal adenosine A_{2A} receptors significantly decreased in rats after intrastriatal injection of quinolinic acid by PET. The PET measurement was validated with both *ex vivo* and *in vitro* autoradiography. [¹¹C]KF18446 PET will provide a new diagnostic tool for characterizing post-synaptic striatopallidal neurons of the striatum.

ACKNOWLEDGMENTS

This work was supported by Grant-in-Aid for Scientific Research (B) No. 10558115 from the Ministry of Education, Science, Sports and Culture, Japan.

REFERENCES

1. Fredholm BB, Abbracchio MP, Burnstock G, Daly JW, Harden TK, Jacobson KA, et al. Nomenclature and classification of purinoceptors. *Pharmacol Rev* 1994; 46: 143–156.
2. Haas HL, Selbach O. Functions of neuronal adenosine receptors. *Naunyn Schmiedebergs Arch Pharmacol* 2000; 362: 375–381.
3. Dunwiddie TV, Masino SA. The role and regulation of adenosine in the central nervous system. *Ann Rev Neurosci* 2001; 24: 31–55.
4. Lewis ME, Patel J, Edley SM, Marangos PJ. Autoradiographic visualization of rat brain adenosine receptors using N⁶-cyclohexyl[³H]adenosine. *Eur J Pharmacol* 1981; 73: 109–110.
5. Goodman RR, Snyder SH. Autoradiographic localization of adenosine receptors in rat brain using [³H]cyclohexyladenosine. *J Neurosci* 1982; 2: 1230–1241.
6. Fastbom J, Pazos A, Palacios JM. The distribution of adenosine A₁ receptors and 5'-nucleotidase in the brain of some commonly used experimental animals. *Neuroscience* 1987; 22: 813–826.
7. Fastbom J, Pazos A, Probst A, Palacios JM. Adenosine A₁ receptors in the human brain: a quantitative autoradiographic study. *Neuroscience* 1987; 22: 827–839.
8. Svenningsson P, Hall H, Sedvall G, Fredholm BB. Distribution of adenosine receptors in the postmortem human brain: an extended autoradiographic study. *Synapse* 1997; 27:

- 322–335.
9. Parkinson FE, Fredholm BB. Autoradiographic evidence for G-protein coupled A₂-receptors in rat neostriatum using [³H]-CGS21680 as a ligand. *Naunyn Schmiedebergs Arch Pharmacol* 1990; 342: 85–89.
10. Johansson B, Fredholm B. Further characterization of the binding of the adenosine receptor agonist [³H]CGS 21680 to rat brain using autoradiography. *Neuropharmacology* 1995; 34: 393–403.
11. Gerfen CR, Engber TM, Mahan LC, Susel Z, Chase TN, Monsma FJ, et al. D₁ and D₂ dopamine receptor-regulated gene expression of striatal and striopallidal neurons. *Science* 1990; 250: 1429–1432.
12. Schiffmann SN, Jacobs O, Vanderhaeghen JJ. Striatal restricted adenosine A₂ receptor (RDC8) is expressed by enkephalin but not by substance P neurons: an *in situ* hybridization histochemistry study. *J Neurochem* 1991; 57: 1062–1067.
13. Pollack AE, Harrison MB, Wooten GF, Fink JS. Differential localization of A_{2a} adenosine receptor mRNA with D₁ and D₂ dopamine receptor mRNA in striatal output pathways following a selective lesion of striatonigral neurons. *Brain Res* 1993; 631: 161–166.
14. Augood SJ, Emson PC. Adenosine A_{2a} receptor mRNA is expressed by enkephalin cells but not by somatostatin cells in rat striatum: a co-expression study. *Mol Brain Res* 1994; 22: 204–210.
15. Martinez-Mir MI, Probst A, Palacios JM. Adenosine A₂ receptors: selective localization in the human basal ganglia and alterations with disease. *Neuroscience* 1991; 42: 697–706.
16. Glass M, Dragunow M, Faull RL. The pattern of neurodegeneration in Huntington's disease: a comparative study of cannabinoid, dopamine, adenosine and GABA_A receptor alterations in the human basal ganglia in Huntington's disease. *Neuroscience* 2000; 97: 505–519.
17. Hurley MJ, Mash DC, Jenner P. Adenosine A_{2A} receptor mRNA expression in Parkinson's disease. *Neurosci Lett* 2000; 291: 54–58.
18. Kurumaji A, Toru M. An increase in [³H]CGS21680 binding in the striatum of postmortem brains of chronic schizophrenics. *Brain Res* 1998; 808: 320–323.
19. Ishiwata K, Noguchi J, Toyama H, Sakiyama Y, Koike N, Ishii S, et al. Synthesis and preliminary evaluation of [¹¹C]KF17837, a selective adenosine A_{2A} antagonist. *Appl Radiat Isot* 1996; 47: 507–511.
20. Noguchi J, Ishiwata K, Wakabayashi S, Nariai T, Shumiya S, Ishii S, et al. Evaluation of carbon-11-labeled KF17837: a potential CNS adenosine A_{2a} receptor ligand. *J Nucl Med* 1998; 39: 498–503.
21. Ishiwata K, Noguchi J, Wakabayashi S, Shimada J, Ogi N, Nariai T, et al. ¹¹C-labeled KF18446: a potential central nervous system adenosine A_{2a} receptor ligand. *J Nucl Med* 2000; 41: 345–354.
22. Ishiwata K, Ogi N, Shimada J, Nonaka H, Tanaka A, Suzuki F, et al. Further characterization of a CNS adenosine A_{2a} receptor ligand [¹¹C]KF18446 with *in vitro* autoradiography and *in vivo* tissue uptake. *Ann Nucl Med* 2000; 14: 81–89.
23. Ishiwata K, Shimada J, Wang WF, Harakawa H, Ishii S, Kiyosawa M, et al. Evaluation of iodinated and brominated

- [¹¹C]styrylxanthine derivatives as *in vivo* radioligands mapping adenosine A_{2A} receptor in the central nervous system. *Ann Nucl Med* 2000; 14: 247–253.
24. Wang WF, Ishiwata K, Nonaka H, Ishii S, Kiyosawa M, Shimada J, et al. Carbon-11-labeled KF21213: a highly selective ligand for mapping CNS adenosine A_{2A} receptors with positron emission tomography. *Nucl Med Biol* 2000; 27: 541–546.
 25. Massieu L, Thedinga KH, McVey M, Fagg GE. A comparative analysis of the neuroprotective properties of competitive and uncompetitive *N*-methyl-D-aspartate receptor antagonists *in vivo*: implications for the process of excitotoxic degeneration and its therapy. *Neuroscience* 1993; 55: 883–892.
 26. Töpper R, Gehrman J, Schwarz M, Block F, Noth J, Kreutzberg GW. Remote microglial activation in quinolinic acid model of Huntington's disease. *Exp Neurol* 1993; 123: 271–283.
 27. Levivier M, Holemans S, Togasaki DM, Maloteaux JM, Brotchi J, Przedborski S. Quantitative assessment of quinolinic acid-induced striatal toxicity in rats using radioligand binding assays. *Neurol Res* 1994; 16: 194–200.
 28. Levivier M, Gash DM, Przedborski S. Time course of the neuroprotective effect of transplantation on quinolinic acid-induced lesions of the striatum. *Neuroscience* 1995; 69: 43–50.
 29. Nakao N, Grasbon-Frodl EM, Widner H, Brundin P. Antioxidant treatment protects striatal neurons against excitotoxic insults. *Neuroscience* 1996; 73: 185–200.
 30. Ishiwata K, Ogi N, Hayakawa N, Umegaki H, Nagaoka T, Oda K, et al. Positron emission tomography and *ex vivo* and *in vitro* autoradiography studies on dopamine D₂-like receptor degeneration in the quinolinic acid-lesioned rat striatum: comparison of [¹¹C]raclopride, [¹¹C]nemonapride and [¹¹C]*N*-methylspiperone. *Nucl Med Biol* 2002; 29: 307–316.
 31. Umegaki H, Ishiwata K, Ogawa O, Ingram DK, Roth GS, Yoshimura J, et al. *In vivo* assessment of adenoviral vector-mediated gene expression of dopamine D₂ receptors in the rat striatum by positron emission tomography. *Synapse* 2002; 43: 195–200.
 32. Halldin C, Stone-Elander S, Farde L, Ehrin E, Fasth KJ, Långsöm B, et al. Preparation of ¹¹C-labelled SCH23390 for the *in vivo* study of dopamine D₁ receptors using positron emission tomography. *Appl Radiat Isot* 1986; 37: 1039–1043.
 33. Ishiwata K, Ishii S, Senda M. An alternative synthesis of [¹¹C]raclopride for routine use. *Ann Nucl Med* 1999; 13: 195–197.
 34. Ishiwata K, Itou T, Ohyama M, Mishina M, Ishii K, Nariai T, et al. Metabolite analysis of [¹¹C]flumazenil in human plasma during PET studies. *Ann Nucl Med* 1998; 12: 55–59.
 35. Paxinos G, Watson C. *The rat brain in stereotaxic coordinates*. 2nd ed., San Diego; Academic Press, Inc., 1986.
 36. Ishiwata K, Hayakawa N, Ogi N, Oda K, Toyama H, Endo K, et al. Comparison of three PET dopamine D₂-like receptor ligands, [¹¹C]raclopride, [¹¹C]nemonapride and [¹¹C]*N*-methylspiperone, in rats. *Ann Nucl Med* 1999; 13: 161–167.
 37. Hayakawa N, Uemura K, Ishiwata K, Shimada Y, Ogi N, Nagaoka T, et al. A PET-MRI registration technique for PET studies of the rat brain. *Nucl Med Biol* 2000; 27: 121–125.
 38. Hume SP, Lammertsma AA, Myers R, Rajeswaran S, Bloomfield PM, Ashworth S, et al. The potential of high-resolution positron emission tomography to monitor striatal dopaminergic function in rat models of disease. *J Neurosci Methods* 1996; 67: 103–122.
 39. Ardekani BA, Braun M, Hutton BF, Kanno I, Iida H. A fully automatic multimodality image registration algorithm. *J Comput Assist Tomogr* 1995; 19: 615–623.
 40. Ishiwata K, Ogi N, Tanaka A, Senda M. Quantitative *ex vivo* and *in vitro* receptor autoradiography using ¹¹C-labeled ligands and an imaging plate: a study with a dopamine-D₂ like receptor ligand [¹¹C]nemonapride. *Nucl Med Biol* 1999; 26: 291–296.
 41. Tarazi FI, Campbell A, Yeghiayan SK, Baldessarini RJ. Localization of dopamine receptor subtypes in corpus striatum and nucleus accumbens septi of rat brain: comparison of D₁-, D₂- and D₄-like receptors. *Neuroscience* 1998; 83: 169–176.
 42. van der Weide J, De Vries JB, Tepper PG, Horn AS. The effects of kainic acid and 6-hydroxydopamine lesions, metal ions and GTP on *in vitro* binding of the D-2 dopamine agonist, [³H]N-0437, to striatal membranes. *Eur J Pharmacol* 1989; 143: 101–107.
 43. Zhang L, Joseph JA, Roth GS. Effect of aging on vulnerability of striatal D₁ and D₂ dopamine receptor-containing neurons to kainic acid. *Brain Res* 1997; 763: 264–266.
 44. Gerfen CR, McGinty JF, Young WS. III. Dopamine differentially regulates dynorphin, substance P, and enkephalin expression in striatal neurons: *In situ* hybridization histochemical analysis. *J Neurosci* 1991; 11: 1016–1031.
 45. Le Moine C, Normand E, Bloch B. Phenotypical characterization of the rat striatal neurons expressing the D₁ dopamine receptor gene. *Proc Natl Acad Sci USA* 1991; 88: 4205–4209.
 46. Tissingh G, Booij J, Winogrodzka A, van Royen EA, Wolters EC. IBZM- and CIT-SPECT of the dopaminergic system in parkinsonism. *J Neural Transm* 1997; 50 (Suppl): 1–7.
 47. Stoessl AJ, Ruth TJ. Neuroreceptor imaging: new developments in PET and SPECT imaging of neuroreceptor binding (including dopamine transporters, vesicle transporters and post synaptic receptor sites). *Curr Opin Neurol* 1998; 11: 327–333.
 48. Thobois S, Guillouet S, Broussolle E. Contributions of PET and SPECT to the understanding of the pathophysiology of Parkinson's disease. *Neurophysiol Clin* 2001; 31: 321–340.
 49. Kase H. New aspects of physiological and pathophysiological functions of adenosine A_{2A} receptor in basal ganglia. *Biosci Biotechnol Biochem* 2001; 65: 1447–1457.
 50. Kelly PAT, Graham DI, McCulloch J. Specific alterations in local cerebral glucose utilization following striatal lesions. *Brain Res* 1982; 233: 157–172.
 51. Kubota R, Yamada S, Kubota K, Ishiwata K, Tamahashi N, Ido T. Intratumoral distribution of fluorine-18-fluorodeoxyglucose *in vivo*: high accumulation in macrophages and granulation tissues studied by microautoradiography. *J Nucl Med* 1992; 33: 1972–1980.